Surface piezoelectricity: Size effects in nanostructures and the emergence of piezoelectricity in non-piezoelectric materials

Shuangxing Dai,[1,a)] Mohamed Gharbi,[2,a)] Pradeep Sharma,[2,b)] and Harold S. Park[1,c)]
[1]*Department of Mechanical Engineering, Boston University, Boston, Massachusetts 02215, USA*
[2]*University of Houston, Houston, Texas 77204, USA*

(Received 21 July 2011; accepted 8 October 2011; published online 21 November 2011)

In this work, using a combination of a theoretical framework and atomistic calculations, we highlight the concept of "surface piezoelectricity," which can be used to interpret the piezoelectricity of nanostructures. Focusing on three specific material systems (ZnO, $SrTiO_3$, and $BaTiO_3$), we discuss the renormalization of apparent piezoelectric behavior at small scales. In a rather interesting interplay of symmetry and surface effects, we show that nanostructures of certain non-piezoelectric materials may also exhibit piezoelectric behavior. Finally, for the case of ZnO, using a comparison with first principles calculations, we also comment on the fidelity of the widely used core–shell interatomic potentials to capture non-bulk electro-mechanical response. © *2011 American Institute of Physics*. [doi:10.1063/1.3660431]

I. INTRODUCTION

Piezoelectric materials have, over time, attracted significant interest because of applications in a broad range of technologies: energy harvesting, sensing, actuation, advanced microscopy, artificial muscles, among others.[42] More recently, attention has focused on exploring the nature of this electromechanical coupling at the nanoscale and the attendant consequences. For example, Wang and co-workers presented seminal work illustrating how electrical energy can be harvested from bent ZnO nanowires using an atomic force microscope (AFM).[33,38] Similar effects were also reported for GaN nanowires.[34] Through exploitation of nanoscale size effects, researchers have also highlighted the notion of creating piezoelectric materials without using piezoelectric materials,[10,11,31] "giant" piezoelectricity in inhomogeneously deformed nanostructures,[21,22] the origins of nanoindentation size effects,[12,13] and renormalized ferroelectric properties,[8] among others.

The phenomenon of flexoelectricity is responsible for some of the size effects discussed in the aforementioned references—in particular, for high permittivity materials. On the other hand, given the sizable fraction of atoms residing at the surface in a typical nanostructure, it is now well appreciated that surface effects play a tremendous role in both renormalization of materials properties as well as lead to (sometimes) fundamentally new phenomena. Especially for low-permittivity dielectrics (e.g., ZnO), surface effects are likely to dominate. Recent experiments[44] and density functional theory (DFT) calculations have found that ZnO nanostructures exhibit apparent piezoelectric constants that can be both larger and smaller than the expected bulk values.[1,19,23,40] Indeed, this deviation of the piezoelectric properties of nanostructures from the bulk values is attributed to surface effects. Atoms near the surfaces have fewer bonding neighbors than atoms in the bulk; this directly impacts the atomic polarization for surface atoms, which in turn should have a direct effect on the piezoelectric properties. Second, atoms at or near surfaces are subject to surface stresses,[4] which can cause substantial deformation,[20,29] and, thus, changes in polarization of the surfaces, even in the absence of any externally applied forces.[1]

In the present work, using a combination of a theoretical framework and atomistic calculations, we highlight the concept of "surface piezoelectricity," which can be used to interpret the piezoelectricity of nanostructures. We focus on three specific materials as examples: ZnO, $SrTiO_3$, and $BaTiO_3$ (BTO_3). In a rather interesting interplay of symmetry and surface effects, we show that nanostructures of certain non-piezoelectric materials may also exhibit piezoelectric behavior. Through our atomistic calculations, we present the so-called surface piezoelectric constants of the two example materials. These can be then be used in the context of continuum theoretical frameworks[32] to solve boundary value problems of interest.

Another key outcome of the current work is the assessment of the ability of classical core–shell interatomic potentials to capture the non-bulk polarization, and thus the piezoelectric properties of nanostructures. *Ab initio* methods have been utilized for many years to calculate the bulk piezoelectric properties of nanostructures (e.g., for ZnO, see Refs. 2, 5, 6, 16, 24, and 25). However, computational expediency motivates the use of empirical interatomic calculations in the intermediate size range (>5 nm), which is often of interest to experimentalists. Furthermore, classical molecular dynamics can easily handle temperature effects including the phenomenon of pyroelectricity, which is difficult to model using *ab initio* techniques. The previous work by Dai *et al.*[7] demonstrated that the widely used polarizable core–shell potentials for ZnO, i.e., those of Binks and Grimes[3] and Nyberg *et al.*,[27] are indeed (when contrasted with first principle calculations) able to reproduce the bulk piezoelectric constants. One of their conclusions was that the presence of

[a)]S. Dai and M. Gharbi contributed equally to this work.
[b)]Electronic mail: psharma@uh.edu.
[c)]Electronic mail: parkhs@bu.edu.

the polarizable shell is essential in capturing the clamped ion contribution to the piezoelectric material constants. The fidelity of these core–shell potentials to capture surface effects is unknown, and such an assessment is also one of the objectives of the current work.

The outline of this paper is as follows. In Sec. II, we briefly summarize an existing theoretical framework of surface piezoelectricity that can be used to connect continuum approaches and atomistic calculations, whereas in Sec. III, we present some general considerations of the surface-piezoelectric tensor (especially as is relevant for the symmetries of interest in our example materials), as well as a theoretical expression for the size-dependent piezoelectric response of a thin film that can be linked with atomistic calculations in a facile manner. In Sec. IV, we present detailed atomistic calculations: both first principles as well as empirical molecular dynamics. Discussion of our results is in Sec. V.

II. THEORETICAL FRAMEWORK FOR SURFACE PIEZOELECTRICITY

In this section, we briefly summarize the work of Shen and Hu,[32] who recently presented a theoretical framework for surface piezoelectricity. The surface internal energy density U_s, as a function of surface strain, surface polarization, and their first gradients may be expanded as follows:

$$U_s(\varepsilon_s, P_s) = U_{s0} + \frac{\partial U_s}{\partial P^s_\alpha} P^s_\alpha + \frac{\partial U_s}{\partial \varepsilon^s_{\alpha\beta}} \varepsilon^s_{\alpha\beta} + \frac{1}{2}\frac{\partial^2 U_s}{\partial P^s_\alpha \partial P^s_\beta} P^s_\alpha P^s_\beta + \frac{1}{2}\frac{\partial^2 U_s}{\partial \varepsilon^s_{\alpha\beta} \partial \varepsilon^s_{\gamma\kappa}} \varepsilon^s_{\alpha\beta}\varepsilon^s_{\gamma\kappa} + \frac{\partial^2 U_s}{\partial \varepsilon^s_{\alpha\beta} \partial P^s_\gamma} \varepsilon^s_{\alpha\beta} P^s_\gamma, \tag{1}$$

where ε_s is the surface strain tensor and P_s is the surface polarization. We can rewrite U_s as:

$$U_s(\varepsilon_s, P_s) = U_{s0} + \omega_\alpha P^s_\alpha + \Gamma_{\alpha\beta}\varepsilon^s_{\alpha\beta} + \frac{1}{2} a^s_{\alpha\beta} P^s_\alpha P^s_\beta + \frac{1}{2} c^s_{\alpha\beta\gamma\kappa}\varepsilon^s_{\alpha\beta}\varepsilon^s_{\gamma\kappa} + \tilde{d}^s_{\alpha\beta\gamma}\varepsilon^s_{\alpha\beta} P^s_\gamma, \tag{2}$$

where U_{s0}, ω_α, $\Gamma_{\alpha\beta}$, $a^s_{\alpha\beta}$, $c^s_{\alpha\beta\gamma\kappa}$, and $\tilde{d}^s_{\alpha\beta\gamma}$ are the surface material constants. In particular, $\tilde{d}^s_{\alpha\beta\gamma}$ represents the surface-piezoelectric third-order tensor.

The linear surface constitutive equations can then be expressed as:

$$\sigma_s = \frac{\partial U_s}{\partial \varepsilon_s}, \quad E_s = \frac{\partial U_s}{\partial P_s}.$$

Then

$$\sigma^s_{\alpha\beta} = \frac{\partial U_s}{\partial \varepsilon^s_{\alpha\beta}} = \Gamma_{\alpha\beta} + c^s_{\alpha\beta\gamma\kappa}\varepsilon^s_{\gamma\kappa} + \tilde{d}^s_{\alpha\beta\gamma} P^s_\gamma,$$
$$E^s_\alpha = \frac{\partial U_s}{\partial P^s_\alpha} = \omega_\alpha + a^s_{\alpha\beta} P^s_\beta + \tilde{d}^s_{\beta\gamma\alpha}\varepsilon^s_{\beta\gamma}, \tag{3}$$

where σ_s and E_s are the surface stress and the surface effective local electric field, respectively. Similarly, the bulk constitutive equations can be written as:[32]

$$\sigma^b_{\alpha\beta} = \frac{\partial U_b}{\partial \varepsilon^b_{\alpha\beta}} = c^b_{\alpha\beta\gamma\kappa}\varepsilon^b_{\gamma\kappa} + \tilde{d}^b_{\alpha\beta\gamma} P^b_\gamma,$$
$$E^b_\alpha = \frac{\partial U_b}{\partial P^b_\alpha} = a^b_{\alpha\beta} P^b_\beta + \tilde{d}^b_{\beta\gamma\alpha}\varepsilon^b_{\beta\gamma}. \tag{4}$$

III. SURFACE-PIEZOELECTRIC TENSOR AND RENORMALIZATION OF PIEZOELECTRIC TENSOR FOR THIN FILMS

For a 3D nanostructure, the bulk piezoelectric tensor, in its most general form, can be represented as a 3×6 matrix in some suitable basis. Analogously, the surface piezoelectric tensor can be represented as a 2×3 matrix. Using the symmetry of the surface stress tensor, we obtain $d^s_{ijk} = d^s_{jik}$. Therefore, the nonzero components of the piezoelectric surface constants are d^s_{11}, d^s_{12}, d^s_{21}, d^s_{22}, d^s_{16}, and d^s_{26}. The matrix expressing the surface-piezoelectric constants in 2D may be extended in 3D where only these aforementioned components remain nonzero. In particular, for the case of hexagonal ZnO (6-mm symmetry) and tetragonal $BaTiO_3$ (4-mm symmetry), where the 3-direction is considered perpendicular to the isotropic surface, all the bulk piezoelectric components are zeros except for d^B_{15}, d^B_{31}, and d^B_{33}. The components of the surface piezoelectric tensor for the (0001) (or $(000\bar{1})$) surfaces are zero. For $(01\bar{1}0)$ (or $(0\bar{1}10)$) surfaces only three components are nonzero (d^S_{15}, d^S_{31}, and d^S_{33}). Similarly for $(10\bar{1}0)$ and $(\bar{1}010)$, only d^S_{24}, d^S_{32}, and d^S_{33} are nonzero. For the latter, we have the following relations: $d^S_{24} = d^s_{15}$ and $d^S_{32} = d^S_{31}$. The internal energy density (incorporating surface contributions) for a rectangular medium of thickness h can be expressed as follows:

$$W = \frac{U^s}{h} + U^b, \tag{5}$$

where U^s is the surface internal energy density function and U^b is the bulk internal energy density function. Then, according to Shen and Hu,[32] the total energy density function can be written in the following form:

$$w = \ldots + \tilde{d}^b_{ijk}\varepsilon^b_{ij} P^b_k + \frac{\tilde{d}^s_{ijk}}{h}\varepsilon^s_{ij} P^s_k = \ldots + \varepsilon_{ij} P_k \left(\tilde{d}^b_{ijk} + \frac{\tilde{d}^s_{ijk}}{h} \right), \tag{6}$$

where Eq. (6) is a direct consequence of the following:

$$\varepsilon^s_{ij} = \varepsilon^b_{ij} = \varepsilon_{ij} \text{ and } P^s_k = P^b_k = P_k.$$

Therefore, the effective piezoelectric coefficient resulting from the surface and bulk contributions can be calculated as:

$$\tilde{d}^{\text{eff}}_{ijk} = \frac{\partial^2 W_{/v}}{\partial \varepsilon_{ij} \partial P_k} = \tilde{d}^b_{ijk} + \frac{\tilde{d}^s_{ijk}}{h}. \tag{7}$$

For an applied strain, the ith polarization component has the following expression:

$$P_i = P^{sp}_i + P^B_i + P^S_i = P^{sp}_i + d^B_{ijk}\varepsilon_{jk} + \frac{d^S_{ijk}}{h}\varepsilon_{jk},$$

where P_i^{sp} is the spontaneous polarization in the ith direction (in case of ferroelectrics), P_i^B and P_i^S are, respectively, the bulk and the surface polarizations contributions, d_{ijk}^B and d_{ijk}^S are, respectively, the bulk and the surface-piezoelectric stress tensor, ε represents the applied strain, and h is the thickness of structure in the z direction. We can then write that

$$\Delta P_i = P_i - P_i^{sp} = d_{ijk}^B \varepsilon_{jk} + \frac{d_{ijk}^S}{h}\varepsilon_{jk} = d_{ijk}^{\text{eff}}\varepsilon_{jk}. \tag{8}$$

We note that the relationship between the surface-piezoelectric constants d_{ijk}^S, which we will calculate in this work, and those ($\tilde{d}_{ijk}^s$) of the Shen formulation in Eq. (3) are $(\varepsilon_{ni} - \delta_{ni})\tilde{d}_{ijk}^s = -\varepsilon_0 d_{njk}^s$, where ε_{ni} is the dielectric tensor.

Thus, Eq. (7) provides an expression for the apparent piezoelectric constant of a thin film duly incorporating surface piezoelectricity. Table I summarizes the polarization vector components expressions for applied uniform strain in different directions, where the numbers 2 and 4 represent the number of contributing surfaces.

The overall recipe to determine all the bulk (d_{31}^B, d_{33}^B, and d_{15}^B) and surface (d_{31}^s, d_{33}^s, and d_{15}^s) piezoelectric unknowns is clear: we can use Eqs. 9(a)–9(b) and evaluate the polarizations with the same applied strain for two thicknesses h_1 and h_2. Solving six equations with six unknowns (Eqs. 9(a) and 9(b) can be combined together by applying the same strain in both directions simultaneously), we can determine all the bulk and the surface-piezoelectric coefficients. Also, to improve accuracy, we can calculate the effective piezoelectric constant, for each case, for different thicknesses and fit the results with the appropriate equation.

IV. ATOMISTIC CALCULATIONS

A. First-principles calculations for bulk ZnO and its (0001) polar surfaces

The first-principles calculations performed in this study are based on density-functional theory implemented in the Quantum Espresso software.[14] For bulk calculations, a k-point sampling of $(6 \times 6 \times 1)$ grid is implemented. However, for slabs with different thicknesses, ranging from 2S (two Zn–O double layers) to 10S (ten Zn–O double layers), a sampling of $(6 \times 6 \times 2)$ was chosen. The structural parameters for the ZnO unit cell have been specified in many research papers; for our study, we used the same parameters employed by Dal Corso *et al.*[6] and Li *et al.*[19]: $a = 3.2595$ Å, $c/a = 1.5974$, and $u = 0.382$, where a and c denote the lattice constants and the dimensionless parameter, and u is the length of the Zn–O bond parallel to the c axis, in units of c. A schematic of wurtzite ZnO with the polar surfaces is shown in Fig. 1.

TABLE I. Induced polarization expressions due to applied uniform strain.

	ΔP_1	ΔP_2	ΔP_3	Eq. no.
$\varepsilon = \varepsilon^\infty e_1 \otimes e_1$	0	0	$\left(d_{31}^B + 2\frac{d_{31}^S}{h}\right)\varepsilon^\infty$	9(a)
$\varepsilon = \varepsilon^\infty e_2 \otimes e_2$	0	0	$\left(d_{31}^B + 2\frac{d_{31}^S}{h}\right)\varepsilon^\infty$	9(b)
$\varepsilon = \varepsilon^\infty e_3 \otimes e_3$	0	0	$\left(d_{33}^B + 4\frac{d_{33}^S}{h}\right)\varepsilon^\infty$	9(c)
$\varepsilon = \varepsilon^\infty e_1 \otimes e_3 \left(d_{15}^B + 2\frac{d_{15}^S}{h}\right)\varepsilon^\infty$		0	0	9(d)
$\varepsilon = \varepsilon^\infty e_2 \otimes e_3$	0	$\left(d_{15}^B + 2\frac{d_{15}^S}{h}\right)\varepsilon^\infty$	0	9(e)
$\varepsilon = \varepsilon^\infty e_1 \otimes e_2$	0	0	0	9(f)

For both the bulk and surface calculations, the plane-wave cutoff of 30 Ry was used. To compute the polarization, we first carried out self-consistent total-energy calculations. Then, the polarization was estimated through the Berry-phase approach.[17,30,36] For the bulk model (infinite periodic crystal), different strains were applied in the z direction to compute d_{33}, and different biaxial strains were applied simultaneously in the x and y directions to compute d_{31}. For the surface case, we simulated thin films where the thicknesses ranged between 2S–10S. To deal with the energy convergence problem induced by polar terminated surfaces (0001) and $(000\bar{1})$ because of dangling bonds, we followed the same method as Li *et al.*[19] Specifically, we replaced the Zn and O atoms lying, respectively, in the (0001) and $(000\bar{1})$ surfaces, with artificially created atoms characterized by new valences numbers (6.5 for O and 11.5 for Zn). The method is well studied and justified by Kresse *et al.*[18] Finally, the slabs were modeled by different supercells, where a vacuum region of about 10 Å was employed. The vacuum region was chosen carefully to avoid wavefunction overlaps and interactions between neighboring supercells. Our calculations show that $d_{33}^B = 1.22\ \text{C/m}^2$ and that $d_{31}^B = -0.59\ \text{C/m}^2$. Both are in good agreement with previous DFT calculations for the bulk piezoelectric constants of ZnO.[6]

B. Empirical core–shell-potential-based atomistic modeling of bulk ZnO and its (0001) polar surfaces

We utilized the Binks and Grimes[3] polarizable core–shell potential for ZnO, for which the potential takes a Buckingham-type form, i.e.,

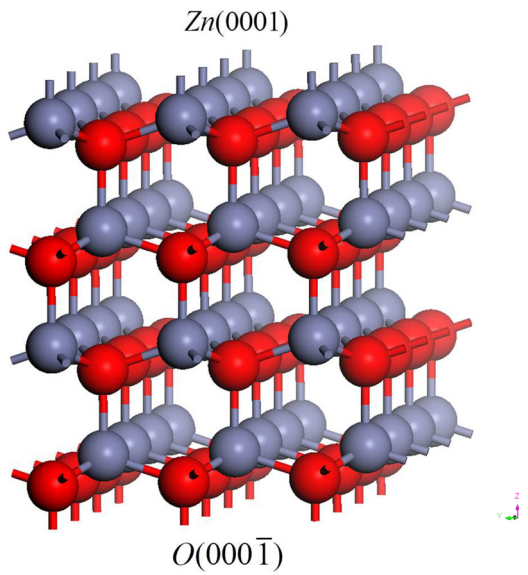

FIG. 1. (Color online) Wurtzite structure of ZnO with polar (0001) Zn- and $(000\bar{1})$ O-terminated surfaces.

$$U(r_{ij}) = \frac{q_i q_j}{r_{ij}} + A\exp\left(\frac{-r_{ij}}{\rho}\right) - \frac{C}{r_{ij}^6}. \quad (10)$$

The first term on the right-hand side of Eq. (10) is the long-ranged Coulombic energy, and the second and third terms represent short-ranged repulsion and attraction, respectively. The bulk piezoelectric constants were previously calculated using both potentials in recent work by Dai *et al.*,[7] giving values of $d_{33}^B = 1.25 \rightarrow 1.29$ C/m^2 and $d_{31}^B = -0.48 \rightarrow -0.54$ C/m^2, which are in good agreement with the current and previous DFT results for ZnO.[6,23,24]

There are two important points that deserve separate mention with regard to using classical polarizable core–shell potentials to calculate the piezoelectric constants of ZnO surfaces. First, because we are interested in the surface properties of ZnO, special care must be taken in calculating the long-ranged Coulombic interactions in Eq. (10), where the Ewald summation technique, which relies upon lattice periodicity, becomes invalid at surfaces. To account for this, we utilized the approach developed by Fennell and Gezelter,[9] who improved the short-ranged charge-neutralization method originally proposed by Wolf *et al.*[39] to provide continuous forces at the potential cut-off distance. For the ZnO crystal, we utilized the Fennell potential parameters of $\alpha = 3.0$ nm^{-1} and the cut-off distance $R_c = 1.0$ nm, as these values led to converged values for the bulk Madelung energy for ZnO, while considering a relatively small interaction radius R_c for computational efficiency.

Second, it is well known that the polar (0001) surfaces of ZnO are unstable, and lead to a non-convergent electrostatic potential with increasing nanofilm size.[18,26,35] Corrections to this non-convergent potential issue have typically relied on surface reconstructions, or charge reduction, where the surface Zn and O atoms take on a reduced charge of +1.5 and −1.5, respectively. The charge reduction can also be understood in terms of the tetrahedral bonding, where, because of the fact that the surface Zn and O atoms have three neighbors instead of four, their charge is reduced proportionally. In the present work, we avoid the non-convergent electrostatic potential by modifying the charges of the surface Zn and O atoms to be 75% of their bulk values, as recently suggested by various authors for classical potentials.[18,26,35]

To calculate the surface-piezoelectric constants using the classical polarizable core–shell potentials, we created thin films of ZnO that were periodic in the plane, with free (0001) surfaces normal to the plane. The surface-piezoelectric constants were calculated in the same manner as the DFT calculations. Specifically, to calculate d_{33}^S, we first allowed the film to relax, then applied strain normal to the plane in the [0001] direction while calculating the corresponding change in polarization with each increment in strain. To calculate d_{31}^S, we first relaxed the film and then biaxially strained the film. The film thickness was kept constant after the initial relaxation to not only ensure convergence to the bulk piezoelectric constant at large film thicknesses, but also to eliminate any strain in the direction normal to the (0001) surface.

C. Comparison between first principles and empirical molecular dynamics results

Our results are based on theoretical formulas introduced in Table I, and computational calculations performed using first-principles code Quantum Espresso and classical molecular statics using the publicly available code GROMACS.[15] The quantum code was validated through calculation of surface energy and comparison with results published by Li *et al.*[19] The surface energy is defined as the difference between the total energies of the film model and the bulk model with the same number of primitive cells divided by the number of the Zn–O double layers. Our calculations show that the surface energies are 2.53 eV (for 2S) and 1.56 eV (for 4*S*) compared to 2.48 eV and 1.52 eV reported by Li *et al.*[19] In the following, we present Fig. 2 for the effective piezoelectric coefficients d_{33}.

To estimate the bulk constant d_{33}^B and the surface constant d_{33}^S, we fit both the DFT and MD results (the same results are plotted in Fig. 2) to the theoretical model ($d_{33}^{\text{eff}} = d_{33}^B + 4(d_{33}^S/h)$) introduced by Eq. 9(c) in Table I. The present study shows that the DFT results give $d_{33}^B = 1.22$ C/m^2 and $d_{33}^S = -0.15 \times 10^{-9}$ C/m compared, respectively, to $d_{33}^B = 1.24$ C/m^2 and $d_{33}^S = -0.125 \times 10^{-9}$ C/m calculated using Li *et al.*'s[19] results. In contrast, the MD results give a surface-piezoelectric constant of $d_{33}^s = -0.32 \times 10^{-9}$ C/m.

The same fitting technique is used to determine the bulk constant d_{31}^B and the surface constant d_{31}^s. Our DFT and MD results shown in Fig. 2 are fitted to the theoretical model ($d_{31}^{\text{eff}} = d_{31}^B + 2(d_{31}^S/h)$) described by Eqs. 9(a) and 9(b) from Table I. The fitting shows that for DFT $d_{31}^B = -0.59$ C/m^2 and $d_{31}^s = 0.1 \times 10^{-9}$ C/m. In contrast, using classical MD, we obtain $d_{31}^s = 0.29 \times 10^{-9}$ C/m. As was the case for the surface piezoelectric constant d_{33}^s, we find that the MD result is larger than the DFT result.

Figure 2 summarizes the effective piezoelectric constants d_{33} for different film thicknesses. It is clear that the MD results are qualitatively similar to the DFT results,

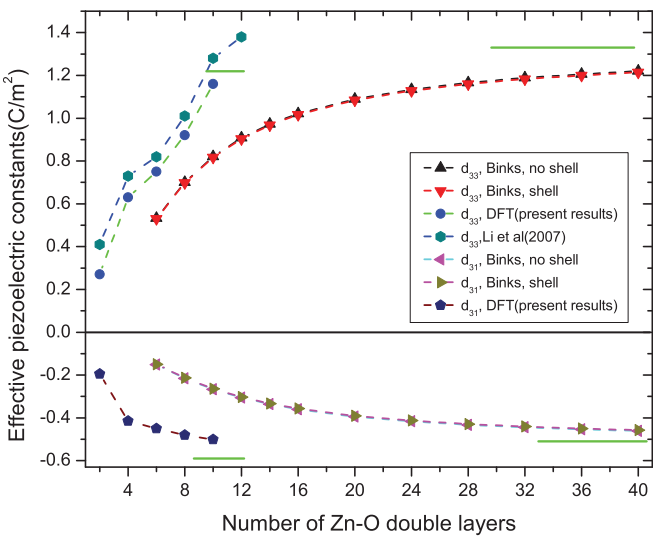

FIG. 2. (Color online) Effective piezoelectric constant d_{33} and effective piezoelectric constant d_{31} vs the number of Zn–O double layers as calculated using both DFT and MD.

though the effective piezoelectric constant is always smaller for the same film thickness. This leads to the surface-piezoelectric constant from MD being larger and more negative than the DFT results. Physically, this implies that the piezoelectric properties as obtained using MD are less bulk-like than those obtained using DFT. We also note that both the MD and DFT results, as expected, converge to the bulk value of d_{33} with increasing film thickness. The MD results, however, converge more slowly. One interesting point is that Fig. 2 demonstrates that in both the present DFT results for d_{33}^{s} and the previous DFT results of Li *et al.*,[19] the value approaches and appears to increase to a value greater than the bulk value for d_{33}^{B}, where in contrast the MD results do not overshoot the bulk value at any point.

Figure 2 also shows different effective piezoelectric constants d_{31} for different thickness ZnO nanofilms. The DFT results are seen again to converge much more quickly to the bulk value of $d_{31}^{B} = -0.59\ \mathrm{C/m^2}$ with increasing nanofilm thickness as compared to the MD results, which again show the same qualitative trend as the DFT results.

The surface-piezoelectric values physically represent the difference in piezoelectric behavior as compared to the reference bulk system, similar to how surface energy is calculated thermodynamically as an excess value with the perfect infinite crystal energy as the reference value.[24] Interpreted in this way, it is clear that the piezoelectric properties of ZnO nanostructures with polar (0001)-type surfaces are (for the cases we studied) always less than the corresponding bulk values. Furthermore, because the MD values are larger than the DFT values for both surface-piezoelectric constants, future MD studies of surface effects on piezoelectricity can be interpreted as exhibiting a stronger deviation from the expected bulk piezoelectric properties than would otherwise be expected based on the present DFT results.

Table II summarizes the comparison between DFT and MD results for both the bulk and surface-piezoelectric constants. Whereas the MD results are equally accurate for the bulk piezoelectric constants, their fidelity suffers when dealing with surfaces, although the established trends are qualitatively correct. Furthermore, it is interesting to note that inclusion of the polarizable shell for the core–shell potentials has an insignificant effect on the surface-piezoelectric properties; this is similar to what was observed previously by Dai *et al.*[7] for the bulk piezoelectric constants, where the shell did enable a non-zero clamped ion term, but did not change the values of the piezoelectric constants appreciably. In this sense, an analogy can be drawn to MD calculations of surface energy or surface stress, where it also is well known that the MD results are qualitatively, and not quantitatively correct when compared to benchmark DFT results.[37] Still, the results are promising as they do suggest that the core–shell interatomic potentials are sufficiently accurate as to be utilized to study size and surface effects on the piezoelectric properties of ZnO nanostructures with polar (0001)-type surfaces.

TABLE II. Comparison between DFT and MD calculations for bulk and surface ZnO piezoelectric constants (d_{33} and d_{31}).

	Bulk values (in $\mathrm{C/m^2}$)			Surface values (in C/m)		
		MD			MD	
	DFT	Shell	No shell	DFT	Shell	No shell
d_{33}	1.22	1.33	1.34	-0.15×10^{-9}	-0.32×10^{-9}	-0.32×10^{-9}
d_{31}	−0.59	−0.51	−0.51	0.10×10^{-9}	0.29×10^{-9}	0.29×10^{-9}

D. Bulk and surface first-principles calculations for piezoelectric $BaTiO_3$

Following the same procedure previously described in Sec. IV A, the effective piezoelectric constants of tetragonal $BaTiO_3$ nanostructures with different thicknesses have been calculated. We used the same DFT tool based on Quantum Espresso algorithms. The bulk calculations are conducted using a k-point sampling of $(6\times6\times1)$ grid. However the slabs with different thicknesses were performed using a sampling of $(6\times6\times2)$ grid. The BTO cell parameters used in our calculations are $a = 3.938$ Å and $c = 3.993$ Å.[28] The plane wave cutoff used for our calculation is 30 Ry. Similar to the ZnO case, we performed both self-consistent total-energy and polarization calculations (based on Berry-phase approach). Also, the slabs were constructed such that a vacuum region of 10 Å was considered. It is shown in Fig. 3 that $d_{33}^{B} = 6.70\ \mathrm{C/m^2}$ and that $d_{31}^{B} = -4.10\ \mathrm{C/m^2}$. Using results from Table I and results plotted in Fig. 3, the surface-piezoelectric constants for tetragonal $BaTiO_3$ are obtained. We found that $d_{33}^{S} = -0.9\times10^{-9}\ \mathrm{C/m}$ and $d_{31}^{S} = 0.7\times10^{-9}\ \mathrm{C/m}$. The bulk piezoelectric constant d_{33}^{B} is in good agreement with results published by Zgonik *et al.*[43] Also, the bulk piezoelectric constant d_{31}^{B} is in good agreement with the constant used by Gharbi *et al.*[13]

E. First-principles calculations for cubic $BaTiO_3$ and $SrTiO_3$: Interplay of symmetry and surface effects in non-piezoelectric materials

The previous results were for a ZnO, which, due to its non-centrosymmetric wurtzite crystal structure, exhibits

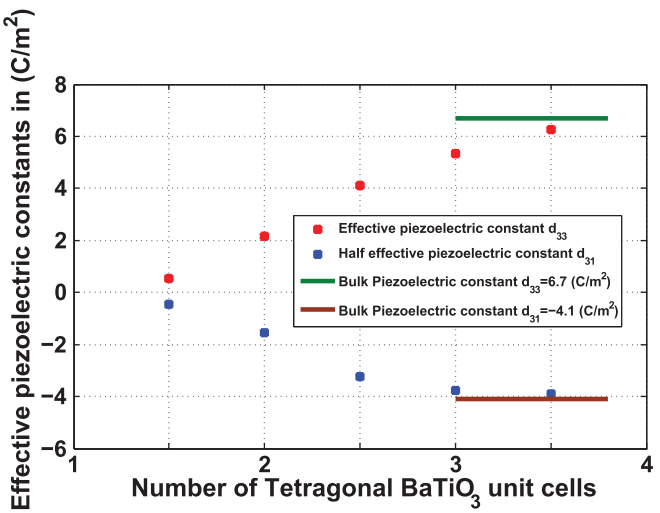

FIG. 3. (Color online) Effective piezoelectric constant d_{33} and effective piezoelectric constant d_{31} vs the number of tetragonal $BaTiO_3$ unit cells as calculated using DFT.

TABLE III. Atomic relaxations (in percent of bulk lattice constant) for $BaTiO_3$ (0001) surface. Positive sign corresponds to outward atomic displacement.

		Displacements					
		δ_x		δ_y		δ_z	
Layer	Ion	Ref. 1	Present study	Ref. 1	Present study	Ref. 1	Present study
1	Ba^{2+}	0	0	0	0	−0.066	−0.022
	O^{2-}	0	0	0	0	−0.038	−0.012
2	Ti^{4+}	0	0	0	0	−0.005	0.008
	O^{2-}	0	0	0	0	−0.016	0.004
	O^{2-}	0	0	0	0	−0.016	0.004
3	Ba^{2+}	0	0	0	0	−0.022	−0.003
	O^{2-}	0	0	0	0	−0.016	−0.002

piezoelectric behavior in bulk form. In contrast, there exist other materials, such as $BaTiO_3$ that show piezoelectricity only in certain temperature ranges (corresponding to appropriate crystal structures). For example, in its cubic form, BTO does not exhibit piezoelectricity. Here, we demonstrate, using DFT calculations, that lattice contraction because of surface stresses can overcome these crystallographic limitations to induce piezoelectric behavior in nanostructures of otherwise non-piezoelectric cubic $BaTiO_3$.

The polarizations are calculated through Berry-phase calculations for cubic relaxed perovskite structures $BaTiO_3$ and $SrTiO_3$ (only one surface is relaxed).[41] We used three different thicknesses 7, 9, and 11 Ba(Sr)–O and Ti–O_2 layers. The surfaces are Ba(Sr)–O terminated surfaces. The relaxation results and the effective piezoelectric constants induced are presented and surface constants are determined and compared to previous results for piezoelectric ZnO and $BaTiO_3$ structures.

We first summarize the surface stress-induced lattice contractions for $BaTiO_3$ in Table III (results for $BaTiO_3$ for seven-layer relaxation), and for $SrTiO_3$ in Table IV (results for $SrTiO_3$ for seven-layer relaxation). As shown in these tables, there is no change in the x and y coordinates for the atoms in the (xy) planes, i.e., there is no relaxation parallel to the free (0001) surface. Therefore, the induced dipole moment for the Ba(Sr)O termination is perpendicular to the surface.

TABLE IV. Atomic relaxations (in percent of bulk lattice constant) for $SrTiO_3$ (0001) surface. Positive sign corresponds to outward atomic displacement.

		Displacements		
		δ_x	δ_y	δ_z
Layer	Ion	Present study	Present study	Present study
1	Sr^{2+}	0	0	−0.010
	O^{2-}	0	0	0.005
2	Ti^{4+}	0	0	0.008
	O^{2-}	0	0	0
	O^{2-}	0	0	0
3	Sr^{2+}	0	0	−0.002
	O^{2-}	0	0	0

TABLE V. Effective piezoelectric constants d_{33}^{eff} (in C/m^2) of the Cubic perovskite nanofilms.

	$BaTiO_3$			$SrTiO_3$		
	7*S*	9*S*	11*S*	7*S*	9*S*	11*S*
$\Delta P\left(10^{-2}\ C/m^2\right)$	0.22	0.18	0.13	0.07	0.05	0.02
$d_{33}^{\text{eff}}\left(C/m^2\right)$	0.22	0.18	0.13	0.07	0.05	0.02

Then

$$\Delta P_3 = d_{33}^{\text{eff}} \varepsilon_{33} = 4\frac{d_{33}^S}{h}\varepsilon_{33}.$$

The polarization calculation and the effective surface constants for $(\varepsilon_{33} = 1\%)$ are shown in Table V for different thickness nanofilms.

The results are fitted to the theoretical equation $d_{33}^{\text{eff}} = 4(d_{33}^S/h)$ and the surface constants are determined for both cases, with the fitted results summarized for both $BaTiO_3$ and $SrTiO_3$ in Table VI compared to the surface-piezoelectric constants previously reported for the ZnO (0001) surface, and the bulk piezoelectric constant for $BaTiO_3$. For cubic $BaTiO_3$, it is shown that the surface relaxation that is summarized in Table III induces an apparent surface-piezoelectric constant in Table VI that is 6% compared to the piezoelectric $BaTiO_3$ surface constant, and is also 33% compared to the piezoelectric ZnO surface constant. The apparent surface-piezoelectric constant given in Table VI for the cubic $SrTiO_3$, due to the surface relaxation that is summarized in Table IV, presents 28% of the value computed for the cubic $BaTiO_3$.

V. DISCUSSION AND SUMMARY

Surfaces in nanostructures play an important role in deciding the nature of electromechanical coupling. We have used a modification of the well-established Gibbsian surface energy theoretical framework to interpret the atomistic results of surface piezoelectricity. Documentation of the surface-piezoelectric constants through atomistics allows a fairly simple calculation of the size-dependent piezoelectric properties for nanostructures. Depending on the material and surface orientation, surfaces can renormalize the piezoelectric constants to be both less than or greater than the corresponding bulk values. In particular, one of our key results is that even non-piezoelectric materials may act as piezoelectric at the nanoscale because of surface effects.

TABLE VI. Comparison with surface constants for piezoelectric and non-piezoelectric structures.

	Piezoelectric ZnO	Piezoelectric $BaTiO_3$	Cubic $BaTiO_3$	Cubic $SrTiO_3$
Surface constant $d_{33}^S(C/m)$	-0.15×10^{-9}	-0.9×10^{-9}	0.050×10^{-9}	0.014×10^{-9}

ACKNOWLEDGMENTS

H.S.P. and S.D. gratefully acknowledge the support of the NSF, Grant No. CMMI-0856261. M.G. and P.S. gratefully acknowledge NSF Grant Nos. CMMI-0708096 and 0826153, and DMR IMI Center: 0844082.

[1]R. Agrawal and H. D. Espinosa, Nano Lett. **11**, 786 (2011).
[2]F. Bernardini, V. Fiorentini, and D. Vanderbilt, Phys. Rev. B **56**, 10024 (1997).
[3]D. J. Binks and R. W. Grimes, Solid-State Commun. **89**, 921 (1994).
[4]R. C. Cammarata, Progress in Surface Science **46**, 1 (1994).
[5]M. Catti, Y. Noel, and R. Dovesi, J. Phys. Chem. Solids **64**, 2183 (2003).
[6]A. Dal Corso, M. Posternak, R. Resta, and A. Baldereschi, Phys. Rev. B **50**, 10715 (1994).
[7]S. Dai, H. S. Park, and M. L. Dunn, Nanotechnology **21**, 445707 (2010).
[8]E. A. Eliseev and A. N. Morozovska, J. Mater. Sci. **44**(19), 5149 (2009).
[9]C. J. Fennell and J. D. Gezelter, J. Chem. Phys. **124**, 234104 (2006).
[10]J. Fousek, L. E. Cross, and D. B. Litvin, Mater. Lett. **39**, 287 (1999).
[11]J. Y. Fu, W. Zhu, N. Li, and L. E. Cross, J. Appl. Phys. **100**, 024112 (2006).
[12]M. Gharbi, Z. H. Sun, P. Sharma, and K. White, Appl. Phys. Lett. **95**, 142901 (2009).
[13]M. Gharbi, Z. H. Sun, K. White, S. El-Borgi, and P. Sharma, Int. J. Solids Struct. **48**, 249 (2011).
[14]P. Giannozzi, S. Baroni, N. Bonini, M. Calandra, R. Car, C. Cavazzoni, D. Ceresoli, G. L. Chiarotti, M. Cococcioni, I. Dabo, A. Dal Corso, S. D. Gironcoli, S. Fabris, G. Fratesi, R. Gebauer, U. Gerstmann, C. Gougoussis, A. Kokalj, M. Lazzeri, L. Martin-Samos, N. Marzari, F. Mauri, R. Mazzarello, S. Paolini, A. Pasquarello, L. Paulatto, C. Sbraccia, S. Scandolo, G. Sclauzero, A. P. Seitsonen, A. Smogunov, P. Umari, and R. M. Wentzcovitch, J. Phys.: Condens. Matter **21**, 395502 (2009).
[15]B. Hess, C. Kutzner, V. D. Spoel, and E. Lindahl, J. Chem. Theory Comput. **4**, 435 (2008).
[16]N. A. Hill and U. Waghmare, Phys. Rev. B **62**, 8802 (2000).
[17]R. D. King-Smith and D. Vanderbilt, Phys. Rev. B **47**, 1651 (1993).
[18]G. Kresse, O. Dulub, and U. Diebold, Phys. Rev. B **68**, 245409 (2003).
[19]C. Li, W. Guo, Y. Kong, and H. Gao, Appl. Phys. Lett. **90**, 033108 (2007).
[20]W. Liang, M. Zhou, and F. Ke, Nano Lett. **5**, 2039 (2005).
[21]M. S. Majdoub, P. Sharma, and T. Cagin, Phys. Rev. B **77**, 125424-1 (2008); **79**, 119904(E) (2009).
[22]M. S. Majdoub, P. Sharma, and T. Cagin, Phys. Rev. B **78**, 121407(R) (2008); **79**, 159901(E) (2009).
[23]A. Mitrushchenkov, R. Linguerri, and G. Chambaud, J. Phys. Chem. C Lett. **113**, 6883 (2009).
[24]Y. Noel, M. Llunell, R. Orlando, P. D'Arco, and R. Dovesi, Phys. Rev. B **66**, 214107 (2002).
[25]Y. Noel, C. M. Zicovich-Wilson, B. Civalleri, P. D'Arco, and R. Dovesi, Phys. Rev. B **65**, 014111 (2002).
[26]C. Noguera, J. Phys.: Condens. Matter **12**, R367 (2000).
[27]M. Nyberg, M. A. Nygren, L. G. M. Pettersson, D. H. Gay, and A. L. Rohl, J. Phys. Chem. **100**, 9054 (1996).
[28]J. Padilla and D. Vanderbilt, Phys. Rev. B **56**,1625 (1997).
[29]H. S. Park, K. Gall, and J. A. Zimmerman, Phys. Rev. Lett. **95**, 255504 (2005).
[30]R. Resta, Rev. Mod. Phys. **66**, 899 (1994).
[31]N. D. Sharma, C. M. Landis, and P. Sharma, J. Appl. Phys. **108**, 024304 (2010).
[32]S. Shen and S. Hu, J. Mech. Phys. Solids **58**, 665 (2010).
[33]J. Song, J. Zhou, and Z. L. Wang, Nano Lett. **6**, 1656 (2006).
[34]W. S. Su, Y. F. Chen, C. L. Hsiao, and L. W. Tu, Appl. Phys. Lett. **90**, 063110 (2007).
[35]P. W. Tasker, J. Phys. C: Solid-State Phys. **12**, 4977 (1979).
[36]D. Vanderbilt and R. D. King-Smith, Phys. Rev. B **48**, 4442 (1993).
[37]J. Wan, Y. L. Fan, D. W. Gong, S. G. Shen, and X. Q. Fan, Model. Simul. Mater. Sci. Eng. **7**, 189 (1999).
[38]Z. L. Wang and J. Song, Science **312**, 242 (2006).
[39]D. Wolf, P. Keblinski, S. R. Phillpot, and J. Eggebrecht, J. Chem. Phys. **110**, 8254 (1999).
[40]H. J. Xiang, J. Yang, J. G. Hou, and Q. Zhu, Appl. Phys. Lett. **89**, 223111 (2006).
[41]X. Y. Xue, C. L. Wang, and W. L. Zhong, Chin. Phys. Lett. **21**, 825 (2004).
[42]J. Yang, Appl. Mech. Rev. **59**(6), 335 (2006).
[43]M. Zgonik, P. Bernasconi, M. Duelli, R. Schlesser, and P. Günter, Phys. Rev. B **50**, 5941 (1994).
[44]M.-H. Zhao, Z. L. Wang, and S. X. Mao, Nano Lett. **4**, 587 (2004).